Quantitative uniqueness of human brain evolution revealed through phylogenetic comparative analysis

Ian F. Miller[a,b,*], Robert A. Barton[c], Charles L. Nunn[b,d]

[a] Ecology and Evolutionary Biology, Princeton University, 106A Guyot Hall, Princeton, NJ 08544-2016, USA

[b] Department of Evolutionary Anthropology, Duke University, 108 Biological Sciences Building, Campus Box 90383, Durham, NC 27708-9976, USA

[c] Evolutionary Anthropology Research Group, Department of Anthropology, University of Durham, South Road, Durham DH1 3LE, UK

[d] Duke Global Health Institute, Duke University, 310 Trent Drive, Durham, NC 27710, USA

*Corresponding author.

E-mail address: ifmiller@princeton.edu

Abstract

While the human brain is clearly large relative to body size, less is known about the timing of brain and brain component expansion within primates and the relative magnitude of volumetric increases. Using Bayesian phylogenetic comparative methods and data for both extant and fossil species, we identified that a distinct shift in brain-body scaling occurred as hominins diverged from other primates, and again as humans and Neanderthals diverged from other hominins. Within hominins, we detected a pattern of directional and accelerating evolution towards larger brains, consistent with a positive feedback process in the evolution of the human brain. Contrary to widespread assumptions, we found that the human neocortex is not exceptionally large relative to other brain structures. Instead, our analyses revealed a single increase in relative neocortex volume at the origin of haplorrhines, and an increase in relative cerebellar volume in apes.

Keywords: brain evolution, phylogenetic comparative methods, human evolution, primate

Introduction

Primates vary almost a thousand-fold in endocranial volume – a measure which closely approximates brain size – ranging from 1.63 mL in mouse lemurs [1] to 1478 mL in humans [2]. Body size is perhaps the most important statistical predictor of brain size across primates, with larger bodied species having larger brains, but substantial variation remains after accounting for the effects of body size [1]. While numerous comparative studies have sought to identify ecological, behavioral, and cognitive correlates of this variability [3–7], much less is known about the evolutionary patterns and processes that generated extant variation in brain size within the primate clade, how these differ for different components of the brain, or the degree to which the brain phenotypes of particular species, such as humans, are the result of exceptional patterns of evolutionary change.

A common approach to investigating human uniqueness is to test whether humans fall "significantly" far from a regression line, for example by regressing brain size on body mass [8–10]. One surprising recent result reported from such an analysis is that the mass of the human brain is only 10% greater than expected for a primate of human body mass [8]. However, such non-phylogenetic methods may give misleading results because they fail to incorporate trait co-variation among species that results from shared evolutionary history. Valid analysis requires methods that account for phylogeny both when estimating scaling parameters and when evaluating deviations from such scaling exhibited by individual species [11–13]. An additional source of error arises if the species being investigated is included in the regression model [e.g. 8], particularly when, as for humans, the phenotypic trait lies at the extreme of the distribution for the other species in

56 the analysis. This procedure would reduce the magnitude of deviations from expected
57 trait values for lineages that have undergone exceptional change, and in the case of
58 humans, would bias the results toward failing to detect uniqueness.
59 Comparative methods make it possible to incorporate phylogeny into analyses and
60 to model phenotypic evolution in ways that uncover hitherto hidden patterns. Such
61 methods are now being applied to a wide variety of traits [e.g. 13–15], including brain
62 size. Pagel [14] estimated phylogenetic scaling parameters to characterize the
63 evolutionary trajectory of endocranial volume (ECV) in fossil hominins. His analyses
64 revealed that ECV evolution accelerated towards the present. As this analysis did not
65 account for body size, it is not clear to what extent this pattern reflects changes in brain
66 size independent of body size. Montgomery *et al*. [16] used ancestral state reconstruction
67 with fossil data to demonstrate a directional trend in primate brain size evolution and to
68 identify branches in the primate phylogeny along which exceptional evolutionary change
69 occurred. They found that while the absolute change in the mass of the human brain was
70 exceptional, the rate of change relative to body size was not. Phylogenetic methods have
71 also been used to examine how specific brain components evolved and the extent to
72 which the branch leading to humans exhibited unusual amounts or rates of change in the
73 size of these components [17,18]. Recently, Lewitus [19] suggested that comparative
74 analyses of neuroanatomical data can be improved by incorporating and comparing
75 results from different evolutionary models.
76 Here, we use phylogenetic methods to model the evolution of brain size and to
77 identify exceptional evolutionary change along phylogenetic branches. We employ three
78 methods: The first method models trait evolution both as a multi-optima Ornstein-

79 Uhlenbeck (OU) process (which incorporates stabilizing selection and drift) and as a
80 Brownian motion process [20], and then compares the fit of the two models. In cases
81 where the OU model is favored, exceptional patterns of trait evolution are indicated by
82 recent shifts in adaptive optima in humans' (or other species') evolutionary lineage. In
83 cases where the Brownian model is favored, we apply our second method, which is a
84 phylogenetic outlier test that uses phylogenetic generalized least squares (PGLS) to
85 predict a phenotype for a species and then compares observed and predicted values. With
86 this method, we can assess whether humans are a phylogenetic "outlier" relative to
87 expectations based on their phylogenetic position and trait covariation in other primate
88 species. Our last method tests for directional and accelerating evolution by fitting
89 phylogenetic scaling parameters to data on deviation from trait expectations and
90 evolutionary time, building on previous efforts with these approaches [14].
91 Using the first two methods, we investigate the evolution of absolute brain size
92 and brain size relative to body mass within primates. Absolute brain volume has been
93 shown to predict cognitive ability in primates better than other metrics that account for
94 body mass [4,21]. However, brain size is highly correlated with body size [1], and as
95 such it is difficult to interpret the significance of brain size alone. Additionally,
96 accounting for body mass gives more insights into the significance of brain size in life
97 history processes, as relative brain size better approximates relative investment in
98 cognitive ability. Accounting for body mass is also important as the relationship between
99 this trait and brain size is associated with scaling effects that reflect conservation of
100 neural function, such as preservation of somatosensory acuity across large surface areas
101 [22] and compensation for increased neural conduction distances in larger animals

through (i) larger neuron and axon sizes, increased myelination, and increased white matter volume, all of which result in reduced neuron density [23–25] and (ii) increased neural resources devoted to prediction-based sensorimotor control that result from escalating neural conduction delays as body size increases [26]. Other measures of relative brain size such as encephalization quotients, ratios, and residuals have been used in the past, but all make theoretical assumptions about the underlying relationship between brain and body size evolution that may not hold. Using relative measures can bias parameter estimates and is not recommended as a good statistical practice [27]. Instead, an empirical approach is preferred in which the covariation of brain size with body size is accounted for within a statistical model that also accounts for phylogenetic history (such as PGLS).

We also apply the first two phylogenetic comparative methods to investigate the evolution of major brain structures involving the neocortex, cerebellum, and medulla. It is widely assumed that the neocortex expanded disproportionately relative to other brain structures during the evolution of anthropoid primates and most particularly in human evolution [28–30]. Surprisingly however, direct tests of this hypothesis are lacking, despite the focus of much evolutionary and developmental neuroscience on the neocortex as the site of interest for understanding human uniqueness and its developmental mechanisms [31]. Recent evidence suggests that the cerebellum may have contributed more to human brain evolution than previously appreciated: it underwent rapid evolutionary expansion in the great ape clade including hominins [18,32] and has been implicated in shape changes of the brain in hominin fossil endocasts [33,34]. Molecular evidence now corroborates the proposal that selection on cerebellar function was an

important feature of hominoid and hominin brain evolution [35], with changes in protein-coding genes implicated in cerebellar development more likely to have evolved adaptively in apes than those implicated in neocortical development [36]. It therefore appears that the neocortex and cerebellum have had different evolutionary trajectories in primate evolutionary history. More research is needed to document and understand these patterns.

We examined volumetric change in the neocortex and cerebellum relative to both body mass and the volume of the rest of the brain. As a check to establish whether changes in evolutionary patterns for relative neocortex and cerebellum size are primarily attributable to changes in those structures or to changes in the rest of the brain, we investigated the evolution of the rest of the brain relative to body mass. We also conducted analyses of the volume of the medulla relative to body mass and the volume of the rest of the brain. The relative volume of the medulla does not vary significantly across clades [37] and as such it has not been attributed a major role in brain expansion. For the analyses of fossil species, brain component volumes are not available; thus, analyses of these lineages are restricted to overall brain size (ECV).

Although our main focus is on broad patterns across primate phylogeny and on the extent to which human brain evolution fits or departs from these patterns, we also examined brain evolution in other species that are considered to be unusually large-brained, such as the aye-aye (*Daubentonia*) and capuchins (*Cebinae)* [1,38]. Our analyses also help to identify other primate species that have experienced exceptional expansion or reduction of the brain or its components, generating new hypotheses for future research on exceptional brain evolution in primates.

148 We used our third method to characterize patterns of brain evolution in humans
149 and extinct hominins. Pagel [14] conducted similar analyses of raw ECV. Our analyses
150 advance his findings in two ways. First, we incorporate body mass as a predictor.
151 Second, we focus on the deviation from brain size expectations, based on the PGLS
152 methods used to assess outlier status. Our findings therefore provide insights to the
153 evolutionary trajectory of exceptional hominin ECV relative to primate-wide brain-body
154 mass scaling relationships.
155
156 **Methods**
157 Comparative data
158 We compiled ECV and female body mass data on non-human primates [1] as well
159 as humans and fossil hominins [2, Tables 1 and 2]. Given that sex specific body mass
160 estimates are available for ancient humans and extinct hominins [2], we used female
161 values for body mass because female values are more tightly linked to ecological and
162 life-history factors [39] and sexual selection can drive increases in male body mass
163 unlinked to ecology, obscuring brain-body scaling relationships [40]. We also compiled
164 data on neocortex, cerebellum, and medulla volume [18,41,42]. Values used to compute
165 predictor variables (described below) for analyses of brain sub-structures were taken
166 from [1]. We used several phylogenies in our analyses. For analyses of hominin ECV,
167 we constructed a "hominin phylogeny" by combining the hominin consensus tree from
168 [13] and the non-human primate consensus tree from 10kTrees version 3 [43]. To ensure
169 that our results in this set of analyses were not dependent upon the topology of the
170 hominin phylogeny, we repeated them using an "alternate hominin phylogeny,"

171 constructed in a similar manner using another hominin tree from [13]. Details of the tree
172 construction process are given in Appendix 1. In all other analyses we used either the
173 consensus primate phylogeny or a block of 100 primate phylogenies from 10kTrees,
174 version 3.

175 To determine whether patterns of exceptional evolution represent absolute or
176 relative changes in scaling, we included several predictor variables in our analyses. To
177 investigate whether the volumes of structures changed relative to body size, we used
178 body mass as a predictor variable, while we used a "rest-of-brain" metric as a predictor
179 variable to investigate whether the volumes of structures changed relative to other brain
180 structures. For the analyses of all structures other than the medulla, the "rest-of-brain"
181 was computed as whole brain volume – (neocortex volume + cerebellum volume). In
182 analyses of the medulla, we calculated "rest-of-brain" volume as brain volume - medulla
183 volume. We also analyzed the volume of the "rest-of-brain" [whole brain volume –
184 (neocortex volume + cerebellum volume)] relative to body mass. The data sets used in all
185 analyses, along with more detailed descriptions, are given in Appendix 1.

186

187 Table 1: Hominin ECV and body mass data details. All values are from [2].

Species	ECV (mL)	Sample size	Female Body Mass (kg)	Sample size
Australopithecus africanus	464.00	8	30	7
Homo erectus	969.00	40	57	4
Homo habilis	609.00	6	32	2
Homo rudolfensis	726.00	3	51	2
Homo sapiens neanderthalensis	1426.00	23	65	7
Homo sapiens	1478.00	66	57	36
Paranthropus boisei	481.00	10	34	1
Paranthropus robustus	563.00	2	32	2
Australopithecus afarensis	458.00	6	30	4

Table 2: Human brain data

Brain Trait	Source		Notes	Dataset
ECV	1478.00 mL	[2]	Composite of values from 66 fossil specimens from locations across Eurasia and Africa	1
Brain volume	1267.65 mL	[71, calculated from 32, 72-75]	Average of measurements of modern human brains	2
Brain volume	1251.85 mL	Stephan et al. [32]	Measurement of modern human brain	3

Characterizing patterns of phenotypic evolution

We compared the fit of multi-optima Ornstein-Uhlenbeck (OU) models of evolution and Brownian models of evolution using a developmental version of the R package bayou (https://github.com/uyedaj/bayou/tree/537e373b6c15faf6a03f21d3d642d14e567ad4d8) [44,45]. OU models of evolution incorporate stabilizing selection and drift, while Brownian models only include drift. Bayou fits multi-optima OU models to a phylogeny using a Markov-Chain Monte Carlo (MCMC) approach. A shift in selection regime refers to a change in the parameters that determine the optimum trait value (towards which species evolve) at a specific location on a phylogeny. Thus, inferred changes in selective regime provide insights to how lineages differ. Shifts in selection regime along terminal branches of a tree would provide particularly strong evidence for a species' uniqueness.

Grabowski et al. [46] proposed the following OU model to describe the evolution of a trait, y, as a function of a predictor variable, x:

205 Eqn. 1: $dy = -\alpha\,(y - y_0)\,dt + \sigma^2\,dB$

206

207 Eqn. 2: $y_0 = \theta + x\,\beta$

208

209 In these equations, *dy* is the change in the trait value, α is the magnitude of the
210 selective "pull" towards the optimum trait value, y_0, and σ^2 is the variance of the white
211 noise process *dB*. The variables θ and β can be interpreted as the intercept and slope of
212 the optimum regression line specified in Eqn. 2. The optimum regression line represents
213 the state that a species is evolving towards rather than the actual evolutionary trajectory.
214 This model has limited utility when data for *x* are only available for the tips of the
215 phylogeny because the values of *x* must be known along the branches of the phylogeny to
216 infer the expected value of *y* for a lineage. We utilize two similar models implemented in
217 the developmental version of bayou – the unweighted predictor model and the weighted
218 predictor model (corresponding to "immediate" and "alphaweighted" options for
219 "slopechange" in bayou) – as these circumvent the issue of unknown phenotypes in
220 ancestral lineages while incorporating a predictor variable into the OU model. The
221 weighted predictor model considers the evolutionary history of the predictor variable
222 while fitting models, and the unweighted predictor model only considers the values of the
223 predictor variables at the tips of the phylogeny while fitting models. The details of these
224 two models are provided in Appendix 2.
225 Bayou uses a MCMC to parameterize the models to fit the data by inferring the
226 location and magnitude of concurrent shifts θ and β on a phylogeny and by inferring the
227 values of α and σ^2, which remain constant across the phylogeny. The parameters α and

228 σ^2 are used in the calculation of the variance-covariance matrices used in evaluating
229 model fit to the phylogeny. The phylogenetic half-life, the time needed for a trait to
230 evolve halfway to the optimum, is computed as ln(2) / α. We present phylogenetic half-
231 life in units of tree height. A phylogenetic half-life less than tree height indicates that the
232 evolutionary processes can "pull" parameter values to the optimum within the timescale
233 in question, while a phylogenetic half-life that exceeds tree height or constitutes a large
234 percentage of tree height indicates that evolutionary processes have a weak "pull" and
235 trait values are not expected to closely approach the optimum during the timescale in
236 question. The expected variance in trait values evolving to the same optima at
237 equilibrium (stationary variance) can be computed as $\frac{\sigma^2}{2\alpha}$.

238 For each analysis, we ran the weighted and unweighted predictor models. We also
239 ran a Brownian motion model in which the strength of stabilizing selection (α) was fixed
240 at 10^{-6} (resulting in a phylogenetic half-life ~9500x greater than tree height; bayou cannot
241 compute model likelihoods when α is 0), and no shifts away from the root regime were
242 allowed. The predictor variable is still incorporated in the Brownian motion model, but
243 no changes in its coefficient occur on the phylogeny. We used the hominin tree for the
244 analysis of ECV and the consensus tree of extant primates for all other analyses. All
245 MCMCs were run for 5,005,000 time steps, sampling every 10 time steps. The priors
246 used are given in Table 3. For each analysis, two chains were run and checked for
247 convergence in terms of likelihood, α, and σ^2 (see Appendix 3 for discussion of chain
248 non-convergence issues in analyses of ECV). We also checked for correlation in branch-
249 wise posterior shift probability between chains. Diagnostic plots pertaining to chain
250 convergence are given in Source data 1. The two chains were combined, with the first

30% of samples being discarded as burn in. We then obtained the likelihood of each model and calculated Bayes factors for each model pairing [47,48] using the *steppingstone* algorithm in bayou, which implements the method of Fan *et al*. [49]. We imposed a posterior probability cutoff of 0.3 for shift detection.

Model Parameter	Prior Distribution
α	Half-cauchy with scale factor 1. Fixed at 0 in Brownian model.
σ^2	Half-cauchy with scale factor 0.1
β	Normal distribution with standard deviation=0.5, mean=slope of linear model of trait and predictor data
θ	Normal distribution with standard deviation=1, mean=intercept of linear model of trait and predictor data
Number of shifts per branch	Fixed at one
Branch-wise shift probability	Uniform
Number of shifts	Conditional Poisson distribution[1] with mean =0.1*number of edges on phylogeny and maximum=number of edges on phylogeny. Fixed at 0 in Brownian model.
Location of shift along branch	Uniform

Table 3: Priors for bayou MCMC analyses

[1]Calculated using "cdpois" option in bayou.

When the multi-optima OU model was selected over the Brownian motion model, we used the location and magnitude of shifts in adaptive optima to assess changes in patterns of evolution. The inference of a shift on a terminal branch would indicate an exceptional pattern of evolution for a given species.

Ho and Ané [50] identified several potential problems with OU models, including un-identifiability of parameters and over-fitting, but acknowledged that such models may

267 be necessary, and recommended that Bayesian models, specifically bayou, be used to
268 overcome these problems. Several other phylogenetic OU models have been developed
269 (most notably Hansen *et al*. [51]), but none utilized Bayesian parameter estimation.
270 Cooper *et al*. [52] echoed the concerns of Ho and Ané [50] and again recommended using
271 Bayesian approaches. Additionally, they recommended weighing the fit of an OU model
272 of evolution against that of a Brownian model, which do through our model selection
273 process.
274
275 Outlier Detection using PGLS
276 When bayou indicated that the Brownian model of trait evolution was favored over the
277 multi-optima OU model, we conducted a phylogenetic outlier test. This was
278 accomplished using BayesModelS, an R script that generates distributions of predicted
279 trait values for a species or several species based on phylogenetically controlled analyses
280 of trait covariation with predictor variables [53]. BayesModelS uses a Markov-Chain
281 Monte Carlo (MCMC) to fit parameters of a PGLS model and assumes a Brownian
282 motion model of evolutionary change. The PGLS models are used to generate trait value
283 predictions for the species of interest. Uncertainty in phylogenetic structure can be
284 accounted for by sampling from a set of trees [14].
285 BayesModelS accounts for phylogenetic non-independence of residual trait values
286 by incorporating branch scaling factors when fitting PGLS models. The MCMC samples
287 between two branch length scaling factors, λ and κ, to improve the fit of the models. The
288 parameter λ scales the internal branches of the phylogeny and measures phylogenetic
289 signal [54]. Values for λ were constrained to be in the interval [0, 1]. In the κ model

290 phylogenetic tree branch lengths are raised to the power κ. The value of κ has previously
291 been used to assess support for a "speciational" mode of evolution (see Pagel [14]).
292 When predicting the value of a trait for a species (or a group of species), its data
293 were excluded from the BayesModelS analysis to avoid biasing the predictions.
294 BayesModelS was then used to generate a posterior probability distribution of predicted
295 values for that species, based on the predictor variable, estimated phylogenetic signal,
296 and estimated trait co-variation with the other species in the analysis. Species were
297 identified as outliers when their trait value was more extreme than 97.5% of the predicted
298 trait values (i.e. when trait values fell outside 95% credible interval). A species was
299 identified as a positive outlier when its true value fell above the majority of predictions,
300 and a negative outlier when the opposite was true.
301 The analyses conducted using BayesModelS proceeded as follows. First, we
302 investigated whether hominins follow primate brain size to body mass scaling rules by
303 using BayesModelS to predict ECV based on body mass and phylogeny. We tested each
304 hominin species for outlier status while excluding data on all hominins when generating
305 predictions. When computing mean estimates for hominin ECV, we corrected for back
306 transformation bias using the quasi-maximum likelihood estimator method described in
307 [55]. We used the hominin phylogeny or the alternate hominin phylogeny in these
308 analysis, and the data spanned 225 extant primate species (including humans) and 10
309 extinct hominin species.
310 Next, we identified individual primate species that are evolutionary outliers for
311 ECV and other brain structures (neocortex, cerebellum, medulla, rest-of-brain). In these
312 analyses, we accounted for phylogenetic uncertainty by using the block of 100 trees,

313 which included *H. sapiens* and *H. neanderthalensis* but no other hominins. We iteratively
314 tested each species in the data set for outlier status. Our analysis for ECV included data
315 from 145 species, and our analyses for other brain structures structures included data
316 from between 39 and 53 species.

317 MCMC chains were run for 1,000,000 time steps, and the first 200,000 time steps
318 were discarded as burn in. Flat priors were used for all variables being predicted. To
319 assess whether the post-burn in results were drawn from a stable distribution, we used the
320 "heidel.diag" function in the R package coda [56]. When post-burn-in results were not
321 drawn from a stable distribution, we discarded an additional portion of the chain (as
322 indicated by "heidel-diag") so that only results drawn from a stable distribution remained.
323 We ensured that the effective sample sizes for the PGLS model parameters (slope,
324 intercept, most frequently selected phylogenetic scaling parameter) were greater than
325 1000 using the "effectiveSize" function in coda [56]. Details of the MCMC diagnostics
326 are given in supplementary materials S6, along with detailed results concerning the
327 posterior predicted distribution and phylogenetic scaling parameters for each species in
328 each analysis.

329

330 Characterizing the Tempo of ECV Evolution in Hominins

331 We investigated the evolutionary trajectory of brain-body scaling in hominins relative to
332 other primates. We calculated the difference between observed ECV and the mean
333 BayesModelS prediction for brain size (generated in the first described BayesModelS
334 analysis in which data for all hominin species was excluded while generating predictions)
335 for each of the hominin species. This difference, which we call "brain size deviation"

represents the magnitude and direction of the deviation in brain size from what would be expected under primate brain-body scaling rules. We fit four PGLS model to hominin brain size deviation to examine how brain size deviation covaried with the phylogenetic distance from the hominin-*Pan* split: First, we fit a "Brownian" model of brain size deviation with no predictor. We fixed λ at 1 in this and all subsequent models. Next, we fit a "directional" model of brain size deviation predicted by phylogenetic distance from the hominin-*Pan* split, expecting to find a positive relationship between these variables if brain volume relative to body size has increased since the split of hominins and *Pan*. To determine whether evolutionary rates in brain size deviation have accelerated over time, we fit an "acceleration" model that included the phylogenetic scaling parameter δ [14,57]. Values of δ greater than 1 are consistent with accelerating evolution, but not necessarily directional evolution. Finally, we fit a "directional acceleration" model in which we fit the parameter δ and used phylogenetic distance from the hominin-*Pan* split as a predictor of brain size deviation. In this model, a positive relationship between brain size deviation and phylogenetic distance, along with a value of δ greater than 1, would indicate that brain volume relative to body size has increased at an accelerating rate since the divergence of hominins from *Pan*. We compared these models using AICc. Analyses were conducted in the R package caper [58].

Results

Endocranial volume (ECV)

In the bayou analysis of ECV predicted by body mass using the hominin phylogeny, the Brownian model was favored over the weighted and unweighted predictor

359 OU models with Bayes factors greater than 22. When we repeated this analysis using the
360 alternate hominin phylogeny, we found that the un-weighted predictor OU model was
361 favored over the weighted predictor OU model and the Brownian model with Bayes
362 factors greater than 42, despite displaying poor convergence in terms of α and σ^2.
363 However, both chains inferred a similar set of shifts, indicating that this is likely an issue
364 related to parameter identifiability rather than to shift identifiability. In this model,
365 progressive shifts towards larger ECV relative to body mass were detected within the
366 hominin clade along the human lineage (figure 1A,B). Shifts towards larger relative brain
367 size were also detected on the terminal branch leading to *D. madagascariensis* and the
368 internal branches leading to the *Lemuridae* and *Cebinae*, clades, and shifts towards
369 smaller relative brain size were detected on the branch leading to the *Alouatta* clade, the
370 branch leading to the clade containing the *Aotidae* and *Callitrichidae* families, and the
371 branch leading to the *Colobinae* sub-family (figure 1-figure supplement 1). The rejected
372 weighted predictor OU model, as well as both OU models that were rejected in the bayou
373 analysis using the hominin phylogeny, detected a very similar set of shifts that included
374 shifts towards progressively larger ECV relative to body mass along the human lineage
375 (Source data 1). Because the Brownian model was favored in the bayou analysis using
376 the hominin phylogeny, we proceeded with BayesModels analyses using both the

hominin and alternate hominin phylogenies.

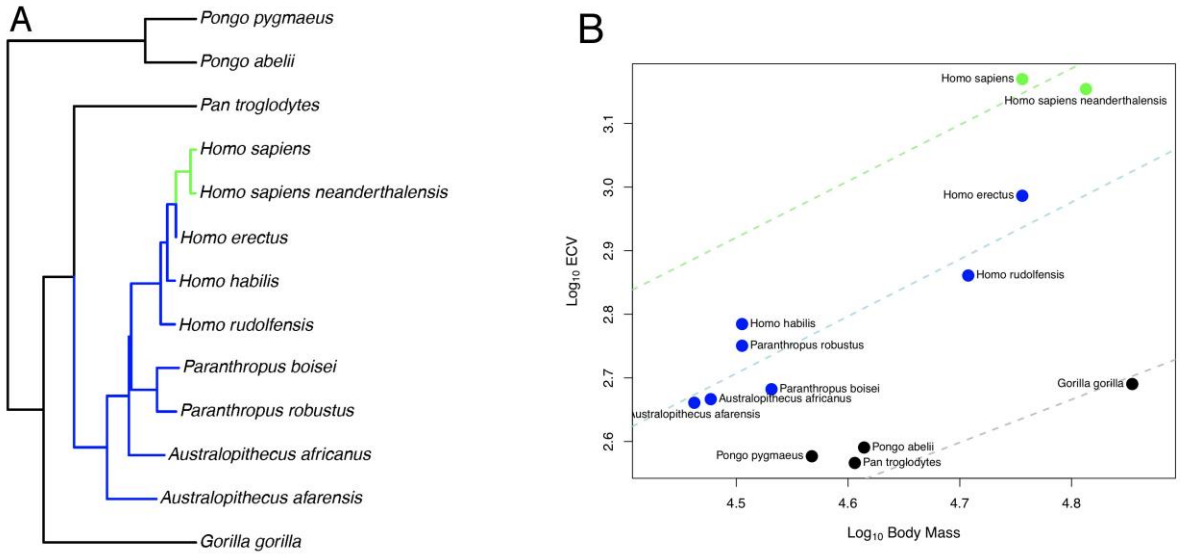

Figure 1: OU Model of ECV Evolution in Primates

Panel A shows the location of the selection regimes identified in an OU model of ECV predicted by body mass. Panel B shows the corresponding optimum regression lines representing the various selection regimes, along with body mass and ECV data. Data are colored by their corresponding selection regimes. All results are from the un-weighted predictor OU model in the bayou analysis using the alternate hominin phylogeny. Only the great ape clade is shown; selection regimes across the entire primate phylogeny are show in figures S1A,B.

In the BayesModelS analysis predicting ECV based on body mass while excluding all hominin data, the observed values for *H*. sapiens and *H*. *neanderthalensis* exceeded the mean values predicted by BayesModelS by 7.63 and 6.96 standard deviations respectively (figure 2C). All hominin species were strongly supported positive outliers, with more than 99.9% of predictions falling below the observed values for ECV. The mean ECV prediction for a primate with the body mass of *H*. *sapiens* was 438 mL. Remarkably, the observed value for humans is 1478 mL, which is 238% greater than the mean of the predicted posterior distribution. A similar result was found for *H*.

395 *neanderthalensis;* the observed ECV for this species exceeded the mean predicted value
396 for a primate of their body mass by 952mL, or 201%. Humans exceeded their predicted
397 ECV by the greatest percentage, but all hominins exceeded predictions by at least 51%
398 (figure 2C, Table 4). We obtained similar results using the alternate hominin phylogeny
399 (figure 2-figure supplement 1, Table 5).

400 When we iteratively predicted ECV based on body mass and phylogeny for each
401 species in the data set (no hominins besides *H. sapiens* and *H. neanderthalensis* were
402 included in this analysis*)* and while using all data to generate predictions. We again found
403 that humans were strongly supported positive outliers (figure 4A). *H. neanderthalensis*
404 was not identified as an outlier, perhaps because these analyses included all species
405 except for the one being predicted, and thus inclusion of *H. sapiens* resulted in a wide
406 posterior distribution when predicting ECV in *H. neanderthalensis*. Indeed, when we
407 excluded *H. sapiens* in this analysis we found that *H. neanderthalensis* was identified as a
408 strongly supported positive outlier (Source data 1). We also identified several other
409 primate species as outliers (see Table 6 and Source data 1).

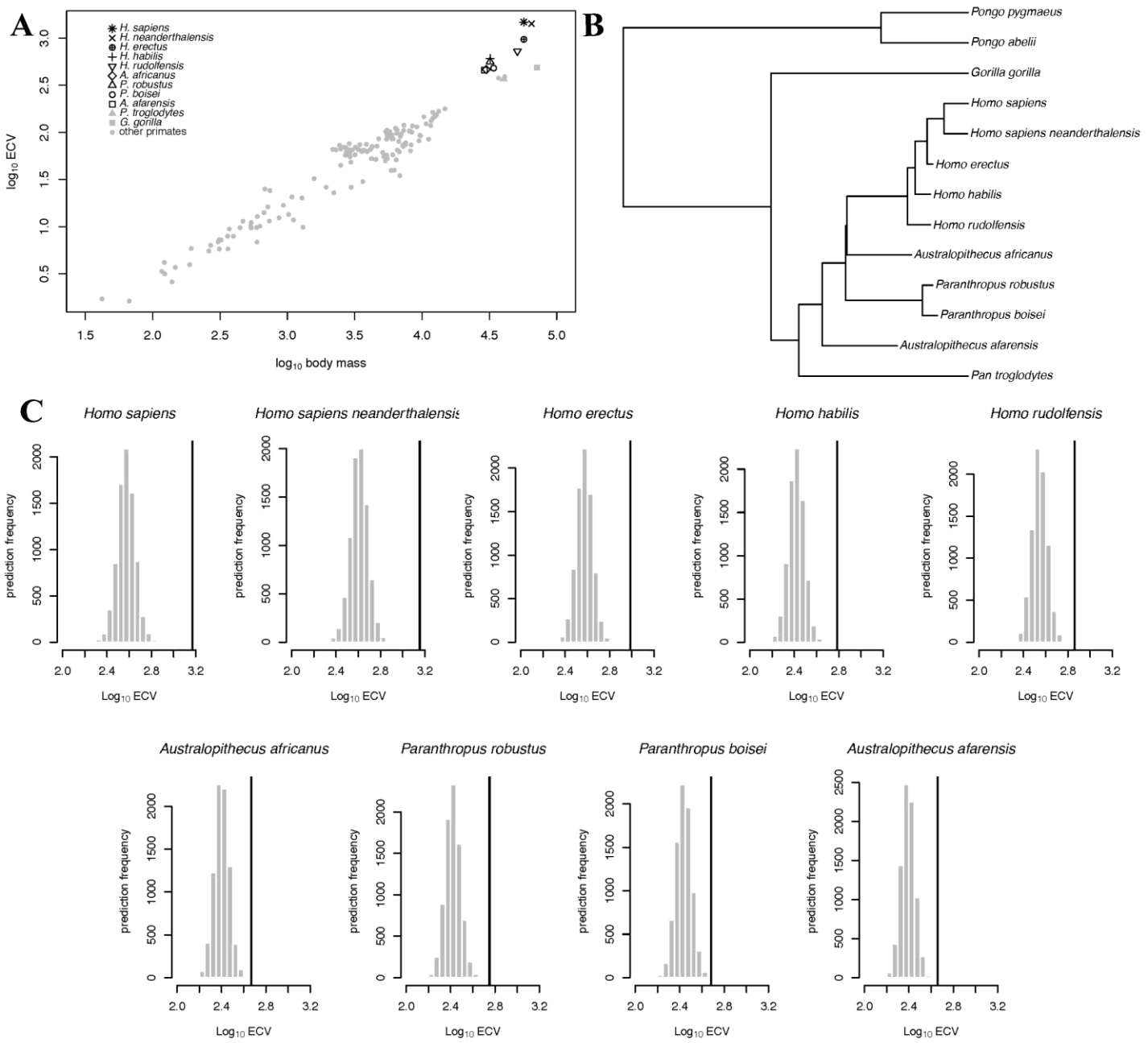

410

411 **Figure 2: BayesModelS predictions of ECV in hominins**

412 Panel A shows a scatter plot of primate ECV and body mass data. Panel B shows the topology of
413 the great ape portion of the hominin phylogeny used in the BayesModelS analyses of hominin
414 ECV. Panel C shows the posterior distributions of predicted ECV values generated by
415 BayesModelS for hominin species with body mass used as the predictor variable. Vertical lines
416 indicated observed values.

417 Table 4: Predicted Hominin ECV values

	true value (ml)	**corrected prediction (ml)**	**difference (ml)**	**% difference**
Australopithecus africanus	464.00	294.73	169.27	57.43
Homo erectus	969.00	438.24	530.76	121.11
Homo habilis	609.00	306.83	302.17	98.48
Homo rudolfensis	726.00	409.63	316.37	77.23
Homo sapiens	1478.00	437.76	1040.24	237.63
Homo sapiens neanderthalensis	1426.00	474.46	951.54	200.55
Paranthropus boisei	481.00	319.00	162.00	50.78
Paranthropus robustus	563.00	307.60	255.40	83.03
Australopithecus afarensis	458.00	288.52	169.48	58.74

418

419 Table 5: Predicted Hominin ECV values from BayesModelS analysis using the alternate
420 hominin phylogeny.
421

	true value (ml)	**corrected prediction (ml)**	**difference (ml)**	**% difference**
Australopithecus africanus	464.00	288.18	175.82	61.00
Homo erectus	969.00	431.04	537.96	124.81
Homo habilis	609.00	300.16	308.84	102.89
Homo rudolfensis	726.00	401.94	324.06	80.62
Homo sapiens	1478.00	431.20	1046.80	242.76
Homo sapiens neanderthalensis	1426.00	468.41	957.59	204.44
Paranthropus boisei	481.00	311.41	169.59	54.46
Paranthropus robustus	563.00	299.74	263.26	87.83
Australopithecus afarensis	458.00	281.59	176.41	62.65

422
423

424

425

426 Table 6: Summary of evidence for exceptional brain evolution among non-human

427 primates

Species/Clade	Exceptional Trait	Evidence
Alouatta	Reduced ECV relative to body mass	Shift in OU model
Aotidae and *Callitrichidae*	Reduced ECV relative to body mass	Shift in OU model
Cacajao calvus	Increased ECV relative to body mass	Outlier Detection
Cebinae	Increased ECV relative to body mass	Shift in OU model
Cebus albifrons	Increased cerebellum relative to body mass	Outlier detection
Chiropotes satanas	Reduced ECV relative to body mass	Outlier Detection
Colobinae	Reduced ECV relative to body mass	Shift in OU model
Daubentonia madagascariensis	Increased ECV relative to body mass	Shift in OU model
Gorilla beringei[a]	Reduced ECV relative to body mass	Outlier Detection
Gorilla gorilla[a]	Reduced neocortex relative to body mass	Outlier Detection
Lemuridae	Increased ECV relative to body mass	Shift in OU model
Loris tardigradus	Reduced medulla relative to the rest of brain	Outlier Detection
Microcebus murinus	Reduced medulla relative to the rest of brain	Outlier Detection
Nasalis larvatus	Reduced neocortex relative to the rest of the brain	Shift in OU model
Otolemur crassicaudatus	Reduced neocortex, cerebellum relative to body mass	Outlier Detection
Pan troglodytes schweinfurthii	Increased ECV relative to body mass	Outlier Detection
Pan troglodytes troglodytes	Reduced ECV relative to body mass	Outlier Detection

428 [a] Only one *Gorilla* species was included in this analysis, i.e. with outlier analyses

429 conducted separately for each *Gorilla* species.

430

In the bayou analysis of ECV with no predictor variable using the hominin phylogeny, the Brownian model was selected over the un-weighted predictor OU models (in which the influence of the predictor was set to 0) with a Bayes factor > 10. No weighted predictor model was run, as it would have been equivalent to the unweighted model given that no predictor variable was incorporated. An equivalent result was found when we repeated the analysis using the alternate hominin phylogeny. We then proceeded with the BayesModelS analysis, iteratively testing the outlier status of each species in the data set. We used the tree block for this analysis, and as such *H. sapiens* and *neanderthalensis* were the only hominins included. We found that neither humans nor Neanderthals were detected as an outlier (figure 4-figure supplement 1, Source data 1), indicating that without correcting for body mass, the variance in ECV across primates is great enough to prevent humans' brains from being detected as exceptionally large.

Evolutionary trajectory of ECV in Hominins

We conducted PGLS analyses of brain size deviation conducted to characterize the evolution of exceptional brain size in hominins (data shown in figure 3). The analyses revealed evidence for both accelerated evolution of brain size deviation and directional evolution towards larger brain size deviations, as indicated by the directional acceleration model (AICc = -23.38) being favored over the acceleration (AICc = -21.93), directional (AICc = -17.56), and Brownian (AICc = -14.58) evolution models. In this best model, there was evidence of directional evolution towards larger brain size relative to body size (slope = 0.04) over time, and of accelerating evolution (δ=8.36). These results suggest that the exceptionality of the human brain evolved recently. We found similar results

when we repeated this analysis using the alternate hominin phylogeny (figure 3-figure supplement 1). These analyses therefore support a model of accelerating evolution towards larger brain volume relative to body mass in *Homo sapiens*.

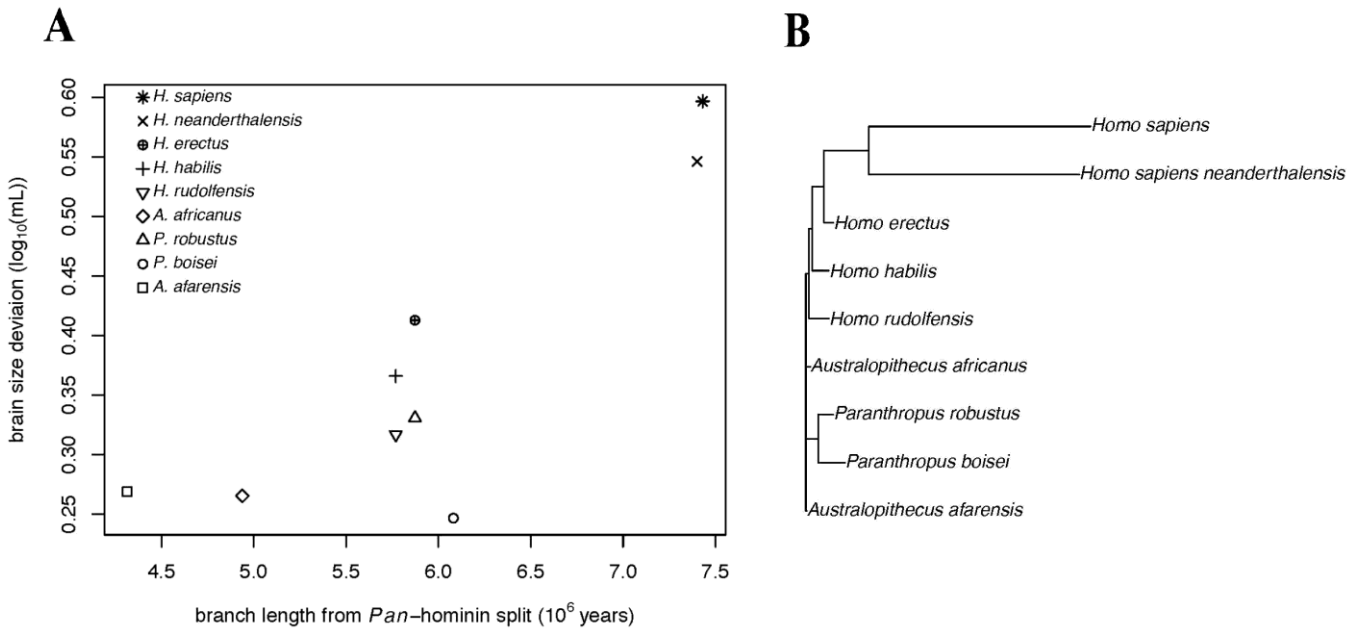

Figure 3: Accelerating Evolution of Brain Size Deviation in Hominins.

A: Brain size deviation was calculated as the difference between the mean BayesModelS prediction (made while excluding all hominin data from analysis and using the hominin phylogeny) and the observed value. Phylogenetic distance was measured as time since the shared ancestor of hominins and *Pan* at 7.43 mya. B: Hominin clade in the hominin phylogeny after δ transformation, with δ=8.36 following the directional acceleration model.

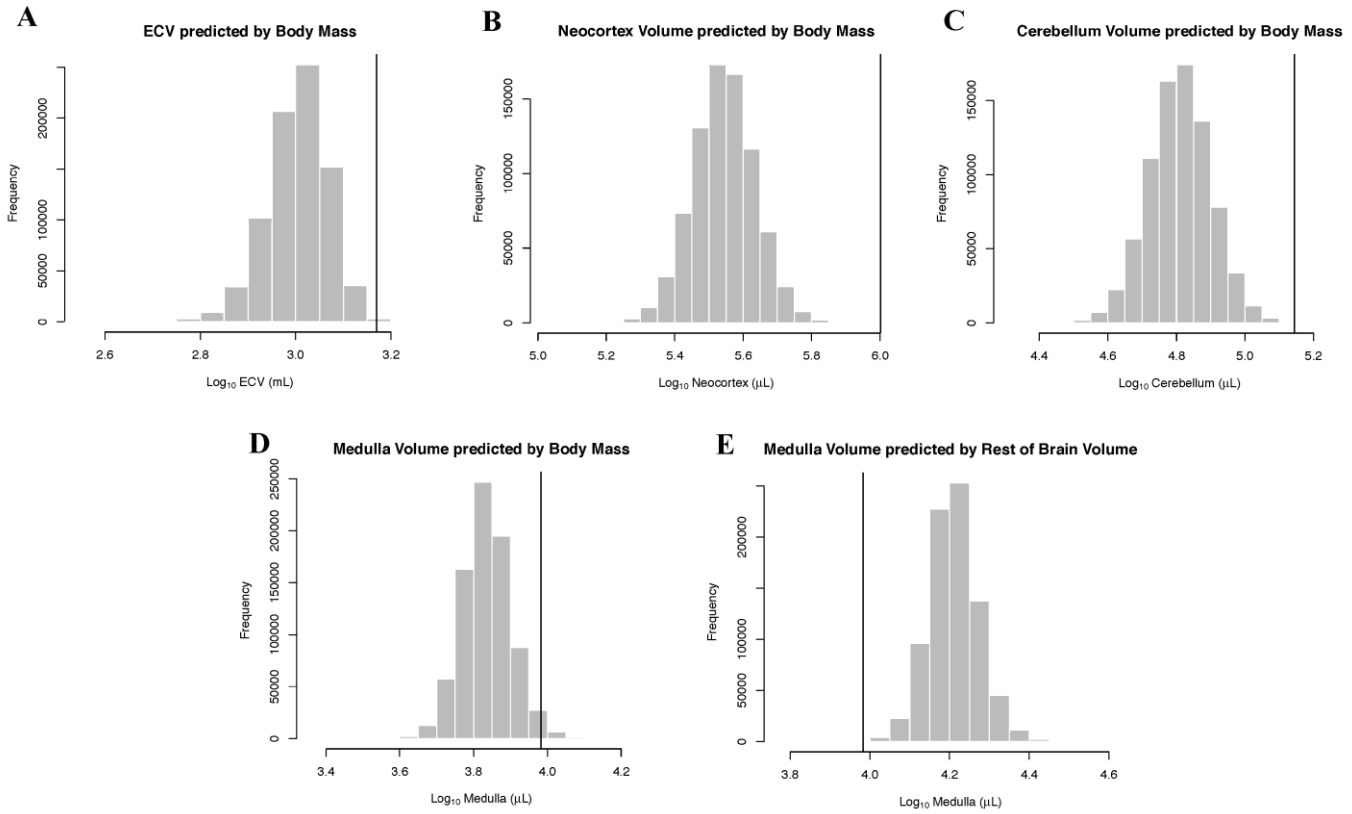

Figure 4: Human Outlier Status for Brain Traits

Predicted distributions of trait values generated by BayesModelS are show as histograms. Vertical bars represent the observed values.

Neocortex

In the bayou analysis of neocortex volume as predicted by body mass, the Brownian motion model was strongly favored over the weighted and unweighted predictor OU models, with Bayes factors > 18. Humans were detected as strongly supported positive outliers for neocortex volume by BayesModelS when body mass was used as the predictor variable (figure 4B).

In the bayou analysis of neocortex volume with "rest-of-brain" as the predictor variable, the weighted predictor model was selected over the unweighted predictor and

Brownian motion models with Bayes Factors > 9.2. In the weighted predictor model, different scaling patterns were detected for strepsirrhines and haplorhines, with the optimum regression line for haplorhines falling above that of strepsirrhines. The only other detected transition in scaling occurred on the terminal branch leading to *Nasalis larvatus*, indicating a shift towards lower relative neocortex size (figure 5A,B).

Cerebellum

In the bayou analysis of cerebellar volume predicted by body mass, the Brownian motion model was favored over the weighted predictor and unweighted predictor OU models, with Bayes factors of 11.96 and 22.79, respectively. BayesModelS identified humans as strongly supported positive outliers for cerebellum volume when body mass was used as the predictor variable (figure 4C).

In the bayou analysis of cerebellum volume relative to the rest-of-brain, the comparison between the unweighted predictor model and the Brownian motion model gave a Bayes factor of 10.65, while the comparison between the unweighted and weighted predictor models gave a Bayes factor of 0.20. This indicates that the OU models clearly outperform the Brownian model, but that neither OU model performs significantly better than the other. Both OU models detected a shift on the branch leading to apes associated with an increase in optimum cerebellar volume relative to the "rest-of-brain" volume (figure 5C,D).

499 Medulla

500 In the bayou analysis of medulla volume predicted by body mass, the Brownian motion
501 model was selected over the two OU models with Bayes factors > 7.4. BayesModelS
502 identified humans as strongly supported positive outliers for medulla volume (figure 4D).
503 No other species were identified as exceptional in this analysis. When medulla was
504 predicted by the "rest-of-brain" volume, the Brownian motion model was again selected
505 over the OU models, with Bayes factors > 3.8. Humans were identified as strongly
506 supported negative outliers (figure 4E).

507

508 Rest-of-brain

509 In the bayou analyses of the rest-of-brain relative to body mass, the OU models were
510 selected over the Brownian motion model, with Bayes factors >13. However, the
511 comparison between the two OU models gave a Bayes factor of 0.20, indicating that
512 neither model is supported relative to the other. No shifts were detected in either model
513 (figure 5E,F).

514

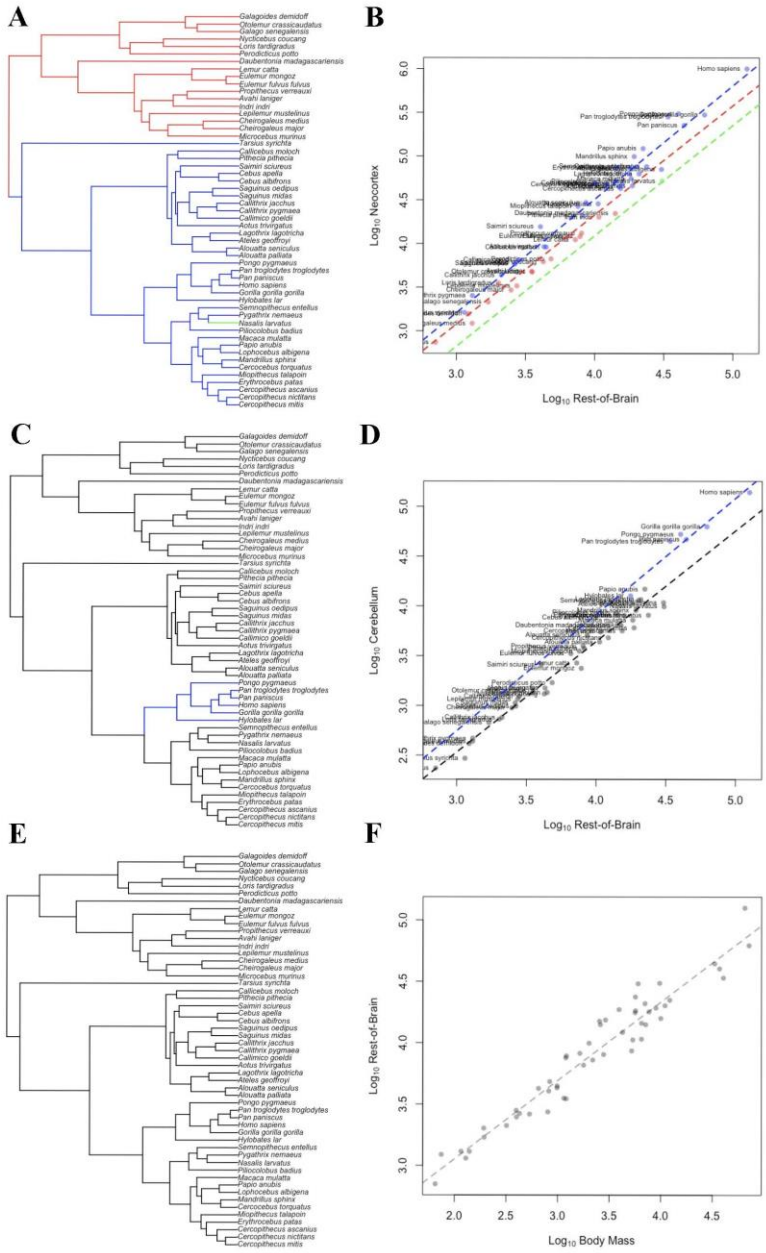

Figure 5: OU Models of Brain Structure Evolution in Primates

A and B correspond to the OU weighted predictor model of neocortex volume predicted by the rest-of-brain. C and D correspond to the OU unweighted predictor model of cerebellum volume predicted by the rest-of-brain. E and F correspond to the OU weighted predictor model of the rest-of-brain volume predicted by body mass. A,C, and E show the location of selection regimes on the primate phylogeny. B,D, and F show the optimum regression lines associated with the selection regimes. Points show primate trait and predictor data; colors correspond to the selection regimes. Colors in A,C, and E match those in B, D, and F.

Discussion

Our phylogenetic analyses revealed that the human brain is 238% larger than the size expected for a primate of similar body mass and phylogenetic position. The exceptional size of the human brain was achieved through progressive scaling shifts towards larger size over several million years of hominin evolution, and the evolution towards increased brain size relative to expectations based on primate scaling patterns accelerated over time. These findings add an important dimension to previous observations of gradual phyletic increases in hominin brain size. Du et al. [59] fit six evolutionary models to within- and between-lineage change in hominin brain sizes (random walk, gradualism, stasis, punctuated equilibrium, stasis-random walk and stasis-gradualism), obtaining the best fit for a gradualism model. However, their non-phylogenetic analysis did not test explicitly for accelerating directional increase. Our findings extend the results obtained by Pagel (2002) on absolute cranial volume, as the pattern of accelerating evolution is found even after accounting for body size. The pattern of accelerating brain size increase documented here is consistent with hypotheses that postulate a co-evolutionary positive feedback process driving human brain evolution, such as feedback between brain size and culture or language [60,61] or between the brain sizes of conspecifics engaged in a socio-cognitive evolutionary arms race [62,63].

While humans clearly have the largest relative brain size among extant primates, anatomically modern humans were closely matched by *H. neanderthalensis*. However, even when accounting for the close phylogenetic relationship between humans and *H. neanderthalensis* and the exceptionally large brain of the latter, the human brain is still much larger than expected: humans were identified as strongly supported outliers when

547 their ECV (relative to body mass) was predicted by phenotypic data from all primates,
548 including *H. neanderthalensis*. This pattern was not reciprocal, however; *H.*
549 *neanderthalensis* was not significantly different from other primates when *H. sapiens* was
550 included in the model.

551 Significant variation exists between estimates of ECV and body mass made from
552 different fossil specimens of the same hominin species [2]. Thus, using single specimens
553 to represent a species would not be a good statistical practice. We used a dataset in which
554 almost all mean species values were calculated from multiple fossil specimens (Table 1).
555 Unfortunately, we could not explicitly account for intraspecific variation in our analyses,
556 as the multi-optima OU model fitting approach and the outlier test are unable to account
557 for variation in both a trait and predictor variable. It would therefore be worthwhile to
558 revisit our analyses as new phylogenetic comparative methods that can account for
559 intraspecific variation become available. Additionally, data quality will likely improve
560 over time. More hominin fossils will be discovered, increasing sample sizes for estimated
561 ECV and body mass.

562 The hominin phylogeny will also likely become better resolved and more
563 complete. We accounted for some phylogenetic uncertainty by repeating our analyses
564 with an alternate phylogeny. The use of different phylogenies influenced outcomes of
565 some statistical tests, as the Brownian model favored when we used the hominin
566 phylogeny and OU model was favored when we used the alternate hominin phylogeny.
567 However, we found that all of the OU models we fit inferred the same pattern of
568 evolution towards larger ECV along the human lineage. The results of our outlier tests
569 and PGLS model fitting – which assume a Brownian mode of evolution – also detected

570 this pattern on different phylogenies. Collectively, these results indicate that our findings
571 are likely to be robust to variations in assumed evolutionary relationships, and potentially
572 to assumptions about the mode of evolution.

573 It is widely assumed that primate brain size evolution in general, and the large
574 size of the human brain in particular, reflects expansion of the neocortex relative to other
575 brain structures [28,64]. Our results contradict this assumption: human neocortical
576 volume was exceptionally large relative to body mass, but not exceptional relative the
577 volume of the rest of the brain. We documented only one shift in neocortex size relative
578 to the rest of the brain during primate evolution: an increase at the origin of all
579 haplorrhines. This shift may be related to the visual specializations of haplorrhines for
580 high-acuity photic vision, mediated by extensive cortical visual areas that make up over
581 50% of the cortex in these species [65–67]. On branches postdating the split between
582 haplorrhines and strepsirrhines, neocortex size is largely predictable from its scaling
583 relationship to the rest of the brain, in line with the proposed importance of cortical-
584 subcortical connectivity in primate brain evolution [68].

585 In contrast, we found that the cerebellum increased in size relative to the rest of
586 the brain on the branch leading to apes. This finding is consistent with the results of
587 recent studies implicating the cerebellum, and especially the lateral cerebellum, in brain
588 expansion in apes and some other mammalian lineages [18,32,69]. Our findings also
589 reinforce the argument that subcortical structures should be given greater consideration in
590 studies of mammalian brain evolution and cognition [23,70]. Cerebellar specialization in
591 apes may have been initiated by the demands on motor control and route-planning
592 imposed by arboreal below-branch locomotion and/or by complex extractive foraging

593 [18,23]. The fact that shifts in the relative size of neocortex and cerebellum occurred on
594 different parts of the tree supports the theory of mosaic brain evolution [71] and suggests
595 that no single adaptive hypothesis is likely to be capable of accounting for primate brain
596 evolution; rather, different selection pressures, on different information-processing
597 capacities, likely operated at different times on different lineages.
598 Consistent with previous studies, we found that the medulla expanded in humans
599 (positive outlier status for medulla volume relative to body mass), but to a lesser degree
600 than other structures (negative outlier status for medulla volume relative to the rest of the
601 brain). Relative to body mass, medulla volume has been shown to be much less variable
602 across taxa than other brain structures, particularly compared to the neocortex and
603 cerebellum. For example, unlike neocortex and cerebellum, medulla volume does not
604 differ significantly between insectivores, strepsirrhines and haplorrhines [37].
605 Accordingly, we found that after controlling for either body mass or brain size, the
606 evolution of the medulla was not modulated by selection towards a stationary optimum in
607 the primate clade. These results further support mosaic brain evolution [71], and also
608 suggest that scaling constraints related to connectivity with other brain regions [72] was
609 less critical for the medulla than for the neocortex and cerebellum.
610 Several non-human primate species exhibited exceptional brain evolution in one
611 trait or another, but only humans showed exceptional brain evolution for multiple brain
612 components. As predicted, we detected shifts towards larger brain size on the terminal
613 branches leading to *D. madagascariensis*, and on the branch leading to the *Cebinae* clade.
614 Large brain size in *Daubentonia* and *Cebinae* has been attributed to extractive foraging
615 and tool use [73–75]. Although not one of our *a priori* expectations, we also documented

616 shifts towards smaller brain size on branches leading to several clades, including
617 *Alouatta*. We also found that two *Gorilla* species exhibit a smaller brain or neocortex size
618 relative to body mass than expected. Given the extremely large body mass of *Gorilla*
619 species, these unique traits may be the byproduct of a body mass increase rather than a
620 reduction in brain size. Also unexpectedly, two *Pan troglodytes* sub-species were found
621 to have exceptionally large and small ECV relative to body mass respectively. However,
622 because more closely related species are weighed more heavily when BayesModelS
623 generates distributions of predicted trait values, sister taxa deviating from expectations in
624 opposite directions could result in both taxa being identified as outliers, even if they both
625 conform to patterns of brain-body scaling for other primates. If the trait distributions for
626 each species overlap significantly, then accounting for intraspecific variation in future
627 analyses could remedy this problem.

628 The unexpected patterns that we observed amongst non-human primates raise
629 several questions for further research. Given the well-established positive correlation
630 between overall brain size and extended life history [76–78], what are the life history
631 implications of mosaic shifts in the sizes of different structures, and do these support any
632 specific interpretations of the correlation between brain size and life histories? One
633 hypothesis, the developmental costs hypothesis, is that large brains simply take longer to
634 grow and mature, leading to extended periods of maternal investment and slower
635 maturation, with other life history correlates of brain size being byproducts of
636 developmental prolongation. Support for this hypothesis is provided by the finding that,
637 amongst mammals, the durations of gestation and lactation have independent effects on
638 pre- and postnatal brain growth, and once these effects are accounted for, other life

639 history correlates are non-significant [79]. Despite their generally correlated evolution
640 [68], we found shifts in the relative size of neocortex and cerebellum on different parts of
641 the phylogenetic tree. Because these two structures have different developmental
642 trajectories, the developmental costs hypothesis predicts different life history correlates;
643 this prediction has now received support [80]. Further work is needed to establish exactly
644 what developmental changes allowed for the neocortex and cerebellum to rest-of-brain
645 scaling rules to change at the origin of haplorrhines and hominoids, respectively.
646 Another area of interest concerns the cases we found of brain or brain component
647 size reduction. Montgomery et al. [16] found that brain size reductions were rare during
648 primate evolution, and that there was a general trend for brain size to increase across
649 multiple branches of the phylogeny. This raises questions for future work concerning the
650 causes, developmental mechanisms and functional implications of specific types of size
651 reduction, such as those that we uncovered in brain size relative to body size in *Alouatta*
652 and other clades, and in neocortex size relative to the rest of the brain in *N. larvatus*.
653 Finally, a key question that has attracted considerable attention concerns the
654 ecological and social drivers of brain size and structure across large-scale evolutionary
655 radiations. It has become increasingly apparent that correlations between overall brain
656 size and behavioral ecology needed to be treated with caution [6,81,82]. However, as
657 suggested by the hypothesis of mosaic brain evolution, correlations between ecology and
658 individual, less functionally heterogenous brain components may be more reliable and
659 robust [18,23,66,67,71,83]. Our analyses focused on gross subdivisions within the brain,
660 and we suggest that further insights could be obtained by applying the phylogenetic
661 methods used in this paper to more fine-grained neuro-anatomical data, using this

approach to tease apart the contributions of correlated and mosaic change among brain components [72] and by incorporating ecological, behavioral, and developmental predictor variables that may account for additional variation in the traits of interest.

In conclusion, we provided robust evidence for directional and accelerating selection towards larger brain size over the course of human evolution, resulting in the human brain being exceptionally large for a primate of similar body mass. We also found that the sizes of human brain components – including the neocortex, cerebellum, and the rest of the brain – are not larger or smaller than expected relative to the size of the rest of the brain, but all are larger than expected for a primate of similar body mass. These results suggest that relative neocortical expansion is not a hallmark of our species. The diversity of evolutionary patterns for various brain components that we observed within primates suggests that no single factor fully explains primate brain evolution; instead, comparative research should investigate how different selection pressures influenced the evolution of different neuroanatomical components at different times on different parts of the phylogenetic tree. Additionally, future work should seek to analyze the evolution of other brain traits, including neuronal composition, using similar phylogenetic comparative methods that account for the non-independence of data from related species.

Competing interests: We have no competing interests to declare.

Acknowledgments: We are grateful to Josef Uyeda for advice on using the developmental version of bayou. We would also like to thank Tom Milledge and Duke Research Computing for assistance with the Duke computing cluster.

686 **Funding:** This work was supported by the National Science Foundation (grant number
687 BCS-1355902)

688 **References:**

689 1. Isler K, Kirk EC, Miller JM, Albrecht GA, Gelvin BR, Martin RD. 2008 Endocranial
690 volumes of primate species: scaling analyses using a comprehensive and reliable data
691 set. *J. Hum. Evol.* **55**, 967–978.

692 2. Robson SL, Wood B. 2008 Hominin life history: reconstruction and evolution. *J.*
693 *Anat.* **212**, 394–425.

694 3. Barton, R.A. 1999 *The evolutionary ecology of the primate brain*. Cambridge:
695 Cambridge University Press.

696 4. MacLean EL *et al*. 2014 The evolution of self-control. *Proc. Natl. Acad. Sci.* **111**,
697 E2140–E2148.

698 5. DeCasien AR, Williams SA, Higham JP. 2017 Primate brain size is predicted by diet
699 but not sociality. *Nat. Ecol. Evol.* **1**, 0112.

700 6. Powell LE, Isler K, Barton RA. 2017 Re-evaluating the link between brain size and
701 behavioural ecology in primates. *Proc. R. Soc. B Biol. Sci.* **284**, 20171765.
702 (doi:10.1098/rspb.2017.1765)

703 7. Noonan MP, Mars RB, Sallet J, Dunbar RIM, Fellows LK. 2018 The structural and
704 functional brain networks that support human social networks. *Behav. Brain Res.*
705 (doi:10.1016/j.bbr.2018.02.019)

706 8. Azevedo FA, Carvalho LR, Grinberg LT, Farfel JM, Ferretti RE, Leite RE, Lent R,
707 Herculano-Houzel S. 2009 Equal numbers of neuronal and nonneuronal cells make
708 the human brain an isometrically scaled-up primate brain. *J. Comp. Neurol.* **513**,
709 532–541.

710 9. De Sousa AA, Sherwood CC, Mohlberg H, Amunts K, Schleicher A, MacLeod CE,
711 Hof PR, Frahm H, Zilles K. 2010 Hominoid visual brain structure volumes and the
712 position of the lunate sulcus. *J. Hum. Evol.* **58**, 281–292.

713 10. Herculano-Houzel S, Kaas JH. 2011 Gorilla and orangutan brains conform to the
714 primate cellular scaling rules: implications for human evolution. *Brain. Behav. Evol.*
715 **77**, 33–44.

716 11. Garland T, Ives, A. R. 2000 Using the Past to Predict the Present: Confidence
717 Intervals for Regression Equations in Phylogenetic Comparative Methods. *Am. Nat.*
718 **155**, 346–364.

719 12. Ross CF, Henneberg M, Ravosa MJ, Richard S. 2004 Curvilinear, geometric and
720 phylogenetic modeling of basicranial flexion: is it adaptive, is it constrained? *J. Hum.*
721 *Evol.* **46**, 185–213.

13. Organ C, Nunn CL, Machanda Z, Wrangham RW. 2011 Phylogenetic rate shifts in feeding time during the evolution of Homo. *Proc. Natl. Acad. Sci.* **108**, 14555–14559.

14. Pagel M. 2002 Modelling the evolution of continuously varying characters on phylogenetic trees. In *Morphology, shape and phylogeny*, Taylor and Francis, 269–286.

15. Vining AQ, Nunn CL. 2016 Evolutionary change in physiological phenotypes along the human lineage. *Evol. Med. Public Health* **2016**, 312–324.

16. Montgomery SH, Capellini I, Barton RA, Mundy NI. 2010 Reconstructing the ups and downs of primate brain evolution: implications for adaptive hypotheses and Homo floresiensis. *BMC Biol.* **8**, 9.

17. Barton RA, Venditti C. 2013 Human frontal lobes are not relatively large. *Proc. Natl. Acad. Sci.* **110**, 9001–9006.

18. Barton RA, Venditti C. 2014 Rapid evolution of the cerebellum in humans and other great apes. *Curr. Biol.* **24**, 2440–2444.

19. Lewitus E. 2018 Inferring Evolutionary Process From Neuroanatomical Data. *Front. Neuroanat.* **12**. (doi:10.3389/fnana.2018.00054)

20. Felsenstein J. 1985 Phylogenies and the comparative method. *Am. Nat.* **125**, 1–15.

21. Deaner RO, Isler K, Burkart J, Van Schaik C. 2007 Overall brain size, and not encephalization quotient, best predicts cognitive ability across non-human primates. *Brain. Behav. Evol.* **70**, 115–124.

22. St. Wecker PG, Farel PB. 1994 Hindlimb sensory neuron number increases with body size. *J. Comp. Neurol.* **342**, 430–438.

23. Barton RA. 2012 Embodied cognitive evolution and the cerebellum. *Philos. Trans. R. Soc. B Biol. Sci.* **367**, 2097–2107. (doi:10.1098/rstb.2012.0112)

24. Wang SS-H, Shultz JR, Burish MJ, Harrison KH, Hof PR, Towns LC, Wagers MW, Wyatt KD. 2008 Functional trade-offs in white matter axonal scaling. *J. Neurosci.* **28**, 4047–4056.

25. Collins CE, Leitch DB, Wong P, Kaas JH, Herculano-Houzel S. 2013 Faster scaling of visual neurons in cortical areas relative to subcortical structures in non-human primate brains. *Brain Struct. Funct.* **218**, 805–816.

26. More HL, Hutchinson JR, Collins DF, Weber DJ, Aung SK, Donelan JM. 2010 Scaling of sensorimotor control in terrestrial mammals. *Proc. R. Soc. Lond. B Biol. Sci.* , rspb20100898.

27. Freckleton RP. 2002 On the misuse of residuals in ecology: regression of residuals vs. multiple regression. *J. Anim. Ecol.* **71**, 542–545.

28. Kriegstein A, Noctor S, Martínez-Cerdeño V. 2006 Patterns of neural stem and progenitor cell division may underlie evolutionary cortical expansion. *Nat. Rev. Neurosci.* **7**, 883–890.

29. Geschwind DH, Rakic P. 2013 Cortical evolution: judge the brain by its cover. *Neuron* **80**, 633–647.

30. Florio M, Huttner WB. 2014 Neural progenitors, neurogenesis and the evolution of the neocortex. *Development* **141**, 2182–2194.

31. Mitchell C, Silver DL. 2017 Enhancing our brains: Genomic mechanisms underlying cortical evolution. In *Seminars in cell & developmental biology*, Elsevier.

32. Smaers JB, Turner AH, Gómez-Robles A, Sherwood CC. 2018 A cerebellar substrate for cognition evolved multiple times independently in mammals. *eLife* **7**, e35696.

33. Kochiyama T *et al*. 2018 Reconstructing the Neanderthal brain using computational anatomy. *Sci. Rep.* **8**, 6296.

34. Neubauer S, Hublin J-J, Gunz P. 2018 The evolution of modern human brain shape. *Sci. Adv.* **4**, eaao5961.

35. Sousa AM *et al*. 2017 Molecular and cellular reorganization of neural circuits in the human lineage. *Science* **358**, 1027–1032.

36. Harrison PW, Montgomery SH. 2017 Genetics of Cerebellar and Neocortical Expansion in Anthropoid Primates: A Comparative Approach. *Brain. Behav. Evol.* **89**, 274–285.

37. Barton RA. 2000 Primate brain evolution: cognitive demands of foraging or of social life. *Move Why Anim. Travel Groups* , 204–237.

38. Pagel M, Harvey P. 1989 Taxonomic differences in the scaling of brain on body weight among mammals. *Science* **244**, 1589–1593. (doi:10.1126/science.2740904)

39. Gordon AD. 2006 Scaling of size and dimorphism in primates II: macroevolution. *Int. J. Primatol.* **27**, 63–105.

40. Fitzpatrick JL, Almbro M, Gonzalez-Voyer A, Hamada S, Pennington C, Scanlan J, Kolm N. 2012 Sexual selection uncouples the evolution of brain and body size in pinnipeds: Brain evolution in pinnipeds. *J. Evol. Biol.* **25**, 1321–1330. (doi:10.1111/j.1420-9101.2012.02520.x)

41. Stephan H, Frahm H, Baron G. 1981 New and revised data on volumes of brain structures in insectivores and primates. *Folia Primatol. (Basel)* **35**, 1–29.

790 42. Bush EC, Allman JM. 2004 The scaling of frontal cortex in primates and carnivores.
791 *Proc*. *Natl*. *Acad*. *Sci*. *U*. *S*. *A*. **101**, 3962–3966.

792 43. Arnold C, Matthews LJ, Nunn CL. 2010 The 10kTrees website: a new online
793 resource for primate phylogeny. *Evol*. *Anthropol*. *Issues News Rev*. **19**, 114–118.

794 44. Uyeda JC, Harmon LJ. 2014 A novel Bayesian method for inferring and interpreting
795 the dynamics of adaptive landscapes from phylogenetic comparative data. *Syst*. *Biol*.
796 **63**, 902–918.

797 45. Uyeda, J.C. 2017. *Bayou developmental version*.
798 https://github.com/uyedaj/bayou/tree/537e373b6c15faf6a03f21d3d642d14e567ad4d8

799 46. Grabowski M, Voje KL, Hansen TF. 2016 Evolutionary modeling and correcting for
800 observation error support a 3/5 brain-body allometry for primates. *J*. *Hum*. *Evol*. **94**,
801 106–116.

802 47. Kass RE, Raftery AE. 1995 Bayes factors. *J*. *Am*. *Stat*. *Assoc*. **90**, 773–795.

803 48. Jeffreys H. 1998 *The theory of probability*. OUP Oxford.

804 49. Fan Y, Wu R, Chen M-H, Kuo L, Lewis PO. 2011 Choosing among Partition Models
805 in Bayesian Phylogenetics. *Mol*. *Biol*. *Evol*. **28**, 523–532.
806 (doi:10.1093/molbev/msq224)

807 50. Ho LST, Ané C. 2013 Asymptotic theory with hierarchical autocorrelation: Ornstein–
808 Uhlenbeck tree models. *Ann*. *Stat*. **41**, 957–981.

809 42. Hansen TF. 1997 Stabilizing selection and the comparative analysis of adaptation.
810 *Evolution **51***, 1341–1351.

811 52. Cooper N, Thomas GH, Venditti C, Meade A, Freckleton RP. 2015 A cautionary note
812 on the use of Ornstein Uhlenbeck models in macroevolutionary studies. *Biol*. *J*. *Linn*.
813 *Soc*. **118**, 64–77.

814 53. Nunn CL, Zhu L. 2014 Phylogenetic prediction to identify "evolutionary
815 singularities". In *Modern Phylogenetic Comparative Methods and Their Application
816 in Evolutionary Biology*, pp. 481–514. Springer.

817 54. Nunn CL. 2011 *The comparative approach in evolutionary anthropology and
818 biology*. University of Chicago Press.

819 55. Smith RJ. 1993 Logarithmic transformation bias in allometry. *Am*. *J*. *Phys*.
820 *Anthropol*. **90**, 215–228. (doi:10.1002/ajpa.1330900208)

821 56. Plummer M, Best N, Cowles K, Vines K. 2006 CODA: convergence diagnosis and
822 output analysis for MCMC. *R News* **6**, 7–11.

57. Pagel M. 1999 Inferring the historical patterns of biological evolution. *Nature* **401**, 877–884.

58. Orme D. 2013 The caper package: comparative analysis of phylogenetics and evolution in R. *R Package Version* **5**.

59. Du A, Zipkin AM, Hatala KG, Renner E, Baker JL, Bianchi S, Bernal KH, Wood BA. 2018 Pattern and process in hominin brain size evolution are scale-dependent. *Proc R Soc B* **285**, 20172738.

60. Wills C. 1993 *The runaway brain: The evolution of human uniqueness*. Basic Books.

61. Deacon TW. 1998 *The symbolic species: The co-evolution of language and the brain*. WW Norton & Company.

62. Dunbar R. 1998 *Grooming, gossip, and the evolution of language*. Harvard University Press.

63. Miller G. 2011 *The mating mind: How sexual choice shaped the evolution of human nature*. Anchor.

64. Rakic P. 2009 Evolution of the neocortex: a perspective from developmental biology. *Nat. Rev. Neurosci.* **10**, 724–735.

65. Drury HA, Van Essen DC, Anderson CH, Lee CW, Coogan TA, Lewis JW. 1996 Computerized mappings of the cerebral cortex: a multiresolution flattening method and a surface-based coordinate system. *J. Cogn. Neurosci.* **8**, 1–28.

66. Barton RA. 1998 Visual specialization and brain evolution in primates. *Proc. R. Soc. Lond. B Biol. Sci.* **265**, 1933–1937.

67. Barton RA. 2007 Evolutionary specialization in mammalian cortical structure. *J. Evol. Biol.* **20**, 1504–1511.

68. Whiting B, Barton R. 2003 The evolution of the cortico-cerebellar complex in primates: anatomical connections predict patterns of correlated evolution. *J. Hum. Evol.* **44**, 3–10.

69. MacLeod C. 2003 Expansion of the neocerebellum in Hominoidea. *J. Hum. Evol.* **44**, 401–429. (doi:10.1016/S0047-2484(03)00028-9)

70. Miller M, Clark A. 2018 Happily entangled: prediction, emotion, and the embodied mind. *Synthese* **195**, 2559–2575. (doi:10.1007/s11229-017-1399-7)

71. Barton RA, Harvey PH. 2000 Mosaic evolution of brain structure in mammals. *Nature* **405**, 1055–1058.

855 72. Montgomery SH, Mundy NI, Barton RA. 2016 Brain evolution and development:
856 adaptation, allometry and constraint. *Proc R Soc B* **283**, 20160433.

857 64. Kaufman JA, Ahrens ET, Laidlaw DH, Zhang S, Allman JM. 2005 Anatomical
858 analysis of an aye-aye brain (Daubentonia madagascariensis, primates: Prosimii)
859 combining histology, structural magnetic resonance imaging, and diffusion-tensor
860 imaging. The Anatomical Record Part A **287**, 1026–1037.

861 74. Melin AD, Young HC, Mosdossy KN, Fedigan LM. 2014 Seasonality, extractive
862 foraging and the evolution of primate sensorimotor intelligence. *J*. *Hum*. *Evol*. **71**,
863 77–86.

864 75. Parker ST. 2015 Re-evaluating the extractive foraging hypothesis. *New Ideas*
865 *Psychol*. **37**, 1–12.

866 76. Isler K, van Schaik CP. 2009 The expensive brain: a framework for explaining
867 evolutionary changes in brain size. *J*. *Hum*. *Evol*. **57**, 392–400.

868 77. Sol D. 2009 Revisiting the cognitive buffer hypothesis for the evolution of large
869 brains. *Biol*. *Lett*. **5**, 130–133.

870 78. González-Lagos C, Sol D, Reader SM. 2010 Large-brained mammals live longer. *J*.
871 *Evol*. *Biol*. **23**, 1064–1074.

872 79. Barton RA, Capellini I. 2011 Maternal investment, life histories, and the costs of
873 brain growth in mammals. *Proc*. *Natl*. *Acad*. *Sci*. , 201019140.

874 80. Powell LE, Street SE, Barton RA. 2019 Maternal investment, life histories, and the
875 evolution of brain structure in primates. *bioRxiv* , 513051. (doi:10.1101/513051)

876 81. Healy SD, Rowe C. 2007 A critique of comparative studies of brain size. *Proc*. *R*.
877 *Soc*. *Lond*. *B Biol*. *Sci*. **274**, 453–464.

878 82. Wartel A, Lindenfors P, Lind J. 2018 Whatever You Want: Inconsistent Results Is
879 The Rule, Not The Exception, In The Study Of Primate Brain Evolution. *bioRxiv* ,
880 454132.

881 83. Barton RA, Purvis A, Harvey PH. 1995 Evolutionary radiation of visual and olfactory
882 brain systems in primates, bats and insectivores. *Philos*. *Trans*. *R*. *Soc*. *Lond*. *B*. *Biol*.
883 *Sci*. **348**, 381–392. (doi:10.1098/rstb.1995.0076)

884 84. Araújo A, Arruda M, Alencar A, Albuquerque F, Nascimento M, Yamamoto M. 2000
885 Body weight of wild and captive common marmosets (Callithrix jacchus). *Int*. *J*.
886 *Primatol*. **21**, 317–324.

887 85. Smith RJ, Jungers WL. 1997 Body mass in comparative primatology. *J*. *Hum*. *Evol*.
888 **32**, 523–559.

889 86. Thalmann U, Geissmann T. 2000 Distribution and Geographic Variation in the
890 Western Woolly Lemur (Avahi occidentalis) with Description of a New Species (A.
891 unicolor. *Int*. *J*. *Primatol*. **21**, 915–941.

892 87. Mounier A, Caparros M. 2015 The phylogenetic status of Homo heidelbergensis – a
893 cladistic study of Middle Pleistocene hominins. *BMSAP* **27**, 110–134.
894 (doi:10.1007/s13219-015-0127-4)

895 88. Barton RA, Venditti C. 2014 Rapid evolution of the cerebellum in humans and other
896 great apes. *Curr*. *Biol*. **24**, 2440–2444.

897 89. MacLeod CE, Zilles K, Schleicher A, Rilling JK, Gibson KR. 2003 Expansion of the
898 neocerebellum in Hominoidea. *J*. *Hum*. *Evol*. **44**, 401–429.

899 90. Bush EC, Allman JM. 2003 The scaling of white matter to gray matter in cerebellum
900 and neocortex. *Brain*. *Behav*. *Evol*. **61**, 1–5.

901 91. Rilling JK, Insel TR. 1998 Evolution of the cerebellum in primates: differences in
902 relative volume among monkeys, apes and humans. *Brain*. *Behav*. *Evol*. **52**, 308–314.

903 92. Rilling JK, Insel TR. 1999 The primate neocortex in comparative perspective using
904 magnetic resonance imaging. *J*. *Hum*. *Evol*. **37**, 191–223.

905 93. Butler MA, King AA. 2004 Phylogenetic comparative analysis: a modeling approach
906 for adaptive evolution. *Am*. *Nat*. **164**, 683–695.

907

908

Supplementary figure legends

Figure 1-figure supplement 1: OU Model of ECV Evolution in Primates

Results are shown for the un-weighted predictor OU model of ECV predicted by body mass. Figure 1 displays the same results, but only for great apes. Panel A shows the location of the selection regimes. Panel B shows the optimum regression lines representing the various selection regimes, along with body mass and ECV data. Data in panel B are colored according to the corresponding regimes shown in panel A.

Figure 2-figure supplement 1: BayesModelS predictions of ECV in hominins

Panel A shows a scatter plot of primate ECV and body mass data. Panel B shows the topology of the great ape portion of the alternate hominin phylogeny used in the BayesModelS analyses of hominin ECV. Panel C shows the posterior distributions of predicted ECV values generated by BayesModelS for hominin species with body mass used as the predictor variable. Vertical lines indicated observed values. The observed value for *H. sapiens s* exceeded the mean value predicted by BayesModelS by more than seven standard deviations. All hominin species were strongly supported positive outliers, with >99.9% of predictions falling below the observed values for ECV.

Figure 3-figure suppelement 1: Accelerating Evolution of Brain Size Deviation in Hominins (alternate hominin phylogeny).

A: Brain size deviation was calculated as the difference between the mean BayesModelS prediction (made while excluding all hominin data from analysis and using the alternate hominin phylogeny) and the observed value. Phylogenetic distance was measured as time

since the shared ancestor of hominins and Pan at 9.28 mya. B: Hominin portion of the alternate hominin phylogeny after δ transformation, with δ=3.745 following the directional acceleration model. Among the PGLS models fit to this data, the directional acceleration model (AICc = -23.88) was favored, as it outperformed the the Brownian (AICc = -15.71), directional (AICc = -22.12), and accelerating (AICc = -22.38) evolution models. This model gave evidence for both evolution towards larger brain volume relative to body mass (slope = 0.06) and for accelerating evolution (δ=3.745).

Figure 4-figure supplement 1: Human outlier status for ECV

In the BayesModelS analysis of ECV with no predictor variable, humans were not detected as outliers. Results for other species are given in Source data 1. Because BayesModelS requires a predictor variable, we assigned each species a random number for the predictor trait. This resulted in the predictor variable not being included in the PGLS model in ~98% of post burn-in MCMC samples. We discarded the remaining samples that included the predictor in the PGLS model before generating predictions.

949

Appendix 1: Data Compilation

All data and trees used in our analyses are included in the Source data 2 file. We compiled three data sets for our analyses. The first was used for the analyses of endocranial volume (ECV), the second was used for the analyses of the neocortex and cerebellum, and the third was used for the analyses of the medulla.

In the first data set ("data set 1.csv"), we compiled ECV and female body mass values for non-human primates from [1], who compiled their data set in part from Araújo [84], Gordon [39], Smith and Jungers [85], and Thalmann and Geissmann [86]. This dataset was supplemented with fossil data for ancient humans and extinct hominins from Robson and Wood [2]. These authors provided two taxonomies: one that recognized more species of hominins (the "splitting taxonomy"), and another that lumped hominin lineages into fewer taxonomic categories (the "lumping taxonomy"). We extracted values from the splitting taxonomy, except those for *Australopithecus africanus*, which were only available from the lumping taxonomy. We also chose to use values for *Homo erectus (sensu lato)* from the lumping taxonomy, as these values was calculated from fossils attributed to both *H. erectus* and *H. ergaster*, two species that are not differentiated in our phylogeny. We did not include *H. heidelbergensis* in our analyses because its phylogenetic position is unresolved [87]. Sample sizes are given in Table 1. Museum numbers for the specimens used in calculating species mean values are given in Appendix I of [2].

In the second data set ("data set 2.csv"), body mass, neocortical volume, and cerebellar volume for humans and extant non-human primates were compiled from the data set of Barton and Venditti [88]. We also complied brain volumes to use in the

973 calculation of the "rest-of-brain" predictor trait in the analyses of these brain structures.
974 These values were calculated as an average of the values given in [41,89–92]. The second
975 data set was limited to extant primates and included values for 55 species, including
976 humans.

977 The third data set ("data set 3.csv") included body mass, brain volumes, and
978 medulla volumes from Stephan et al. [41]. This data set spanned 41 species.

979 A summary of all human ECV and body mass estimates and the analyses in which
980 they were used is given in Tables 1 and 2.

981 All trait and predictor values were $\log_{10}$ transformed prior to analyses. When
982 differences between component volumes were used in analyses, we calculated the
983 logarithms after subtraction.

984 We used several different phylogenetic trees and tree blocks in our analyses. We
985 constructed a "hominin phylogeny" ("hominin.phylogeny.txt") that included humans,
986 extinct hominins, and extant primates for use in the analyses of hominin ECV (including
987 the analyses of directional and accelerating evolution); this phylogeny was produced by
988 grafting the "combined dataset consensus time tree" of hominin evolution from Organ et
989 al. [13] onto the time-scaled consensus tree of extant primates from version 3 of 10kTrees
990 [43]. We grafted the clade (including the root branch) containing *Pan* and all fossil
991 hominins onto the node at which *Gorilla* diverged from the *Pan* lineage, and then re-
992 scaled this pasted clade so that the human tip lined up with those of extant primates. We
993 also constructed an "alternative hominin phylogeny" ("alt.hominin.phylogney.txt" using
994 the "morphology and molecular graft time tree" from Organ et al. [13]. To construct this
995 tree, we again grafted the clade (including the root branch) containing *Pan* and all fossil

hominins onto the node at which *Gorilla* diverged from the *Pan* lineage, and then shortened the root branch so that the human tip lined up with those of extant primates. We were not able to use this method for constructing the hominin phylogeny because it would have resulted in the branch leading to the clade containing *Pan* and hominins having a negative length. Both hominin phylogenies we constructed include humans, 300 other extant primates, and 13 extinct hominin species. In other analyses, we used a consensus tree ("consensus.tree.txt") of extant primates (for OU model fitting) or a block of 100 primate trees ("tree.block.txt") downloaded from version 3 of 10kTrees [43, for phylogenetic prediction].

Appendix 2: Details of Bayou models

The un-weighted predictor model is described by the following equation:

Eqn. 1 $E[y] = W\ \theta_M + x\ \beta_n$

E[y] is the expected value of a species trait. W and θ_M represent the evolutionary weight matrix and θ matrix described in [93]. W is a 1 x *n* matrix whose entries are the weights given to each of the n selection regimes through which the species of interest evolved. The weight of each regime is dependent upon the phylogeny and the value of α. More recent regimes have greater weights, especially when α is high. θ_M is an *n* x 1 matrix of the θ values of the regimes through which the species of interest evolved. The product of W and θ_M gives the effective θ value for a species that evolved towards the various optimum θ values specified in θ_M. β_n is the β value of the parameter regime at the tip of

1019 the phylogeny. Therefore, in this model, the expected phenotype for a species is a
1020 function of the evolutionarily weighted effective θ value, the coefficient of the predictor
1021 variable of the current selection regime, and the value of the predictor at the tip of the
1022 phylogeny.
1023
1024 The weighted predictor model is described by a similar equation:
1025
1026 Eqn. 2 $E[y] = W\,\theta_M + x\,W\beta_M$
1027
1028 β_M is an *n* x 1 matrix of the optimum β values of the n regimes through which the species
1029 evolved, and is analogous to θ_M. Thus, in this model the expected trait value of each
1030 species is a function of the species evolutionarily weighted effective θ and β values, and
1031 the value of the predictor variable x at the tip of the phylogeny.
1032
1033 **Appendix 3: Problems with MCMC convergence in bayou**
1034 Bayou returned several MCMC chains during the analyses of ECV that did not converge
1035 in terms of likelihood, α, and σ^2. To address this issue, we generated up to six MCMC
1036 chains in each analysis for both for the un-weighted predictor, weighted predictor, and
1037 Brownian models. Several chains with exceptionally high mean likelihood had σ^2 values
1038 approaching zero and very high α values that appeared to be bounded by a maximum
1039 value. We infer from these patterns that the chains were settling on an unrealistic pattern
1040 of evolution with the stationary variance approaching zero. These chains also inferred
1041 shifts erratically; they predicted shifts with posterior probability greater than 0.1 on many

1042 branches, but no shifts had a posterior probability greater than 0.3. We discarded these
1043 chains, and then selected the two chains with the highest mean likelihood for each
1044 analysis for subsequent use.
1045
1046

Additional files

Source code 1. Representative Code.

Representative R code files for the bayou analyses ("representative bayou code.R"), BayesModelS analyses ("representative BayesModels code.R"), and pgls model fitting ("pgls models.R"), are contained in the this file, along with the BayesModelS code ("mult.spec.BayesModelS_v24.R") and other necessary data files.

Source data 1. Bayou and BayesModelS Results Details.

Bayou Results details: Diagnostic plots giving details of chain convergence are provided in the "bayou results summary.html" file along with detailed information on all OU and Brownain motion models for each trait and predictor pair.

BayesModelS Results Details: Details of the BayesModelS results and diagnostic parameters of MCMC chains are given in the "BayesModelS.results.csv" and "BayesModelS.results.hominins.removed.csv" files.

Source data 2. All data and trees used in our analyses.

Contains the following files:

1. data set 1.csv
2. data set 2.csv
3. data set 3.csv
4. consensus.tree.txt
5. tree.block.txt
6. grafted.tree.txt

1070